Application of HPFRCC on Coupling Beams with Bundled Diagonal Reinforcement

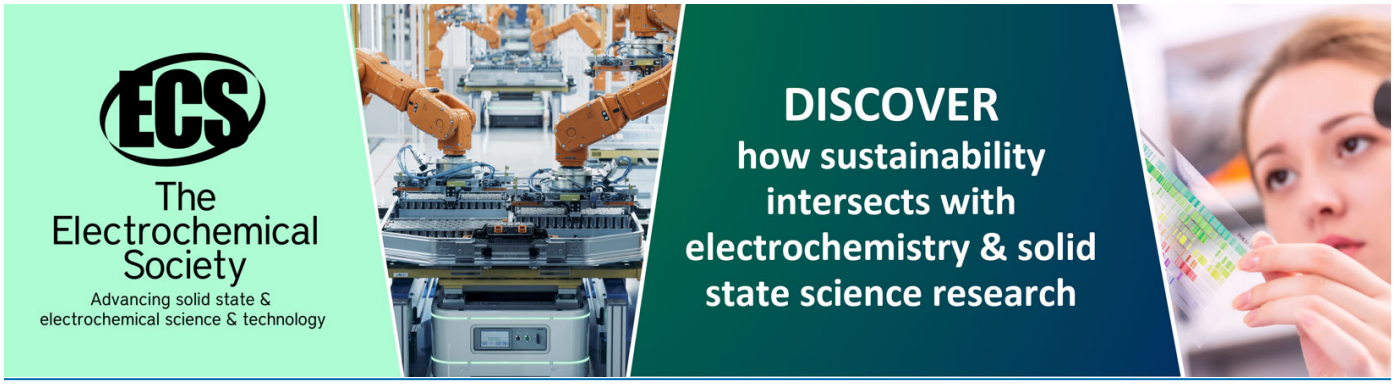

IOP Conf. Series: Materials Science and Engineering **371** (2018) 012034 doi:10.1088/1757-899X/371/1/012034

Application of HPFRCC on Coupling Beams with Bundled Diagonal Reinforcement

SW Han[1], CS Lee[2], KH Lee[3], MS Shin[4]

1 Professor, Department of Architectural Engineering, Hanyang University, Seoul, Korea E-mail: swhan82@gmail.com
2 Graduate Student, Department of Architectural Engineering, Hanyang University, Seoul, Korea
3 Professor, Department of Architectural Engineering, Sejong University, Seoul, Korea
4 Professor, School of Urban and Environmental Engineering, Ulsan National Institute of Science and Technology (UNIST), Ulsan, Korea
E-mail: mtsonicc@naver.com

Abstract. The objective of this study was to develop simple reinforcement details for diagonally reinforced coupling beams; reducing transverse steel by use of high-performance fiber-reinforced cementitious composites (HPFRCCs) and bundling diagonal bars are explored. Four coupling beam specimens with length-to-depth aspect ratios of 2.0 or 3.5 were fabricated and tested under cyclic lateral displacements. The test results revealed that HPFRCC coupling beams with bundled diagonal bars and widely spaced transverse reinforcement (one-half the amount of reinforcement required by current seismic codes.) exhibited excellent seismic performance compared with ordinary concrete coupling beams to bundled diagonal bars and code-required transverse reinforcement.

1. Introduction

Coupling beams reinforced with longitudinal bars parallel to the span of the beam, may experience sliding shear failure near the beam ends at which flexural cracks caused by reversed cyclic loading come across one another [1]. Transverse reinforcement is not capable of preventing sliding shear failure when flexural cracks propagate across the entire depth of the beam between stirrups [2]. Many studies have been conducted with the aim of resolving this problem. Paulay and Binney [3] first developed diagonal reinforcement for coupling beams. Diagonally reinforced coupling beams strongly resist sliding and have ductility, energy dissipation, and stiffness retention capacities superior to those conventionally reinforced coupling beams [4, 5, 6].

According to Harries et al. [7], the confinement option provided in ACI 318-14 [8] is practically difficult to construct when the average shear stress in the beam is greater than $0.5\sqrt{f'_c}$ MPa, where f'_c is the concrete compressive strength in MPa, especially near the mid-span of the beam, where horizontal crossties conflict with diagonal bars.

In efforts to resolve the difficulty of fabricating diagonal reinforcement in coupling beams, various reinforcing details have been investigated and proposed to date [4, 9] Han et al. [9] recently tested the efficiency of bundled diagonal reinforcement in reinforced concrete (RC) coupling beams. Bundled diagonal reinforcement allows more internal space, enhancing workability and allowing simple construction, compared with code-specified diagonal reinforcement in which spacers are needed to

maintain the gaps between separate diagonal bars. Bundling also increases the angle of diagonal reinforcement measured from the longitudinal axis of the beam, thereby increasing both flexural and shear strength. Han et al. [8] reported that coupling beams having bundled diagonal reinforcement achieved greater strength and energy dissipation than, and a similar displacement ductility to, those with code-specified diagonal reinforcement.

Several researchers [10-14] have reported that the use of high performance fiber-reinforced cement composites (HPFRCCs) in structural members improved their seismic resistance. HPFRCCs produce strain-hardening behaviour in uniaxial tension by developing numerous micro-cracks with the assistance of a small portion of engineered fibers [15]. HPFRCCs generally show much higher ductility than normal concrete, under both tension and compression. Thus, the use of HPFRCC may relieve the confinement requirements of members with highly congested reinforcement [10]. When subjected to seismic forces, HPFRCCs are deemed to improve energy dissipation by means of fiber bridging over micro-cracks and excellent bonding between the reinforcing steel and cement within the composite [15].

The aim of the present work was to investigate the effect of HPFRCC on the hysteretic behaviour of coupling beams with bundled diagonally reinforcement. For this purpose, four specimens were made and tested.

2. Experimental Program

2.1. Specimen details

Figure 1 illustrates the dimensions and reinforcing details of the specimens. All specimens were reinforced with bundled diagonal reinforcement and also used the second confinement option illustrated in Fig. 1c.

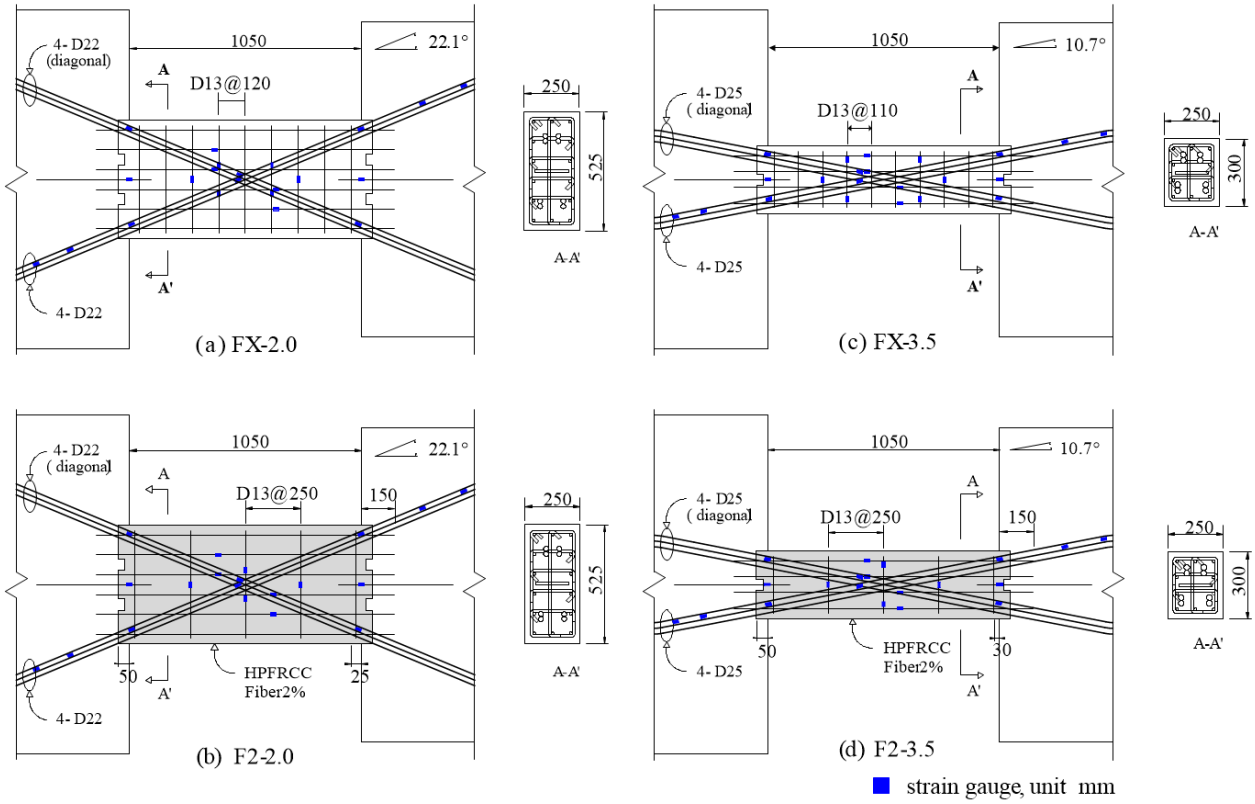

Figure 1. Dimensions and reinforcing details of coupling beam specimens.

The main test variables were the use of conventional RC or the use of HPFRCC in combination with reduced transverse reinforcement, and the use of two different length-to-depth aspect ratios (l_n/h). Table 1 summarizes the test variables and specimen dimensions. The HPFRCC used in this study

contained polyvinyl alcohol (PVA) fibers. The PVA fiber content in the HPFRCC was 2% by volume. The reduced amount of transverse reinforcement was about one half that required by ACI 318-141 [8]. The beam aspect ratio (defined as the span length divided by the total depth of the beam) was selected to be either 2.0 or 3.5 to respectively represent typical deep or slender coupling beams in high-rise residential buildings [14].

The beam length was 1050 mm in all specimens, and the beam depth was 525 mm or 300 mm. The total area of diagonal bars was determined so that the average shear stress in the coupling beam would be limited to approximately $0.5\sqrt{f'_c}$ MPa. The spacing of transverse reinforcement was 120 and 110 mm in the specimens with the aspect ratios of 2.0 and 3.5 respectively, not exceeding six times the diagonal bar diameter as required in ACI 318-14. The inclination angles of bundled diagonal reinforcement in the specimens with the aspect ratios of 2.0 and 3.5 were about 22.1 ° and 10.7 °, respectively. ACI 318-14 specifies that horizontal reinforcement in diagonally reinforced coupling beams mainly used to provide anchorage for horizontal crossties, shall not develop the yield strength at walls. In this study, the embedment length of horizontal reinforcement into the top and bottom stubs was 50 mm in all specimens.

To prevent any damage to the stubs, they were built using concrete of a compressive strength of 60 MPa and included ample reinforcement details.

Table 1. Specimen details and test variables

Specimen	Material	Width (mm)	Depth (mm)	Span length (mm)	Length-to-depth ratio (l_n/h)	Angle α (◦)	Transverse reinforcement spacing (mm)
RC-2.0	RC	250	525	1050	2.0	22.1	120
HC-2.0	HPFRCC	250	525	1050	2.0	22.1	250
RC-3.5	RC	250	300	1050	3.5	10.7	110
HC-3.5	HPFRCC	250	300	1050	3.5	10.7	250

2.2 Loading Frame, Protocol, and Measurements

Figure 2 illustrates the test setup and loading protocol. The test setup was intended to represent the behavior of coupling beams subjected to lateral loading. The coupling beam was arranged vertically, and the steel frame rigidly connected to the top stub was loaded horizontally by a hydraulic actuator. The bottom stub was fixed to the strong floor with anchors. In order to enforce zero moment at the mid-span of the coupling beam, the axis of the actuator was arranged to pass through the mid-span. Also, two roller supports were installed near the ends of the steel frame to prevent the top stub from rotation and vertical translation but allow horizontal translation. Stoppers were installed at the ends of the bottom stub to prevent the specimen from sliding.

Quasi-static reversed cyclic loading was applied with controlled displacement as shown in Fig. 4b The drift ratio is defined as the lateral displacement between the ends of the coupling beam divided by the beam length. For each drift ratio, two same-drift consecutive cycles were applied to assess strength and stiffness degradations. The same loading protocol was used in all tests.

2.3 Material tests

Compression and uniaxial (direct) tension tests were conducted to examine the properties of the normal concrete and HPFRCC used to construct the coupling beam specimens. PVA fibers in the HPFRCC were 2.0% by volume. The water/PCM ratio was approximately 20%, where “PCM” stands for dry premixed cement mortar consisting of binder, fillers, and chemical admixtures. Table 2 summarizes the physical properties of the PVA fibers used in the HPFRCC. In the normal concrete, the maximum aggregate size was 25 mm, whereas the HPFRCC contained neither coarse nor fine aggregates.

For the compression tests, three cylindrical specimens having 100 mm in diameter and 200 mm in

height were fabricated according to ASTM C39, and cured under the same condition as the coupling beam specimens. Three LVDTs in parallel were installed around the perimeter of the specimen in the loading direction to estimate the average compressive strain, with the gage length of approximately 90 mm.

Fig. 3a shows the compressive stress-strain curves of the HPFRCC and normal concrete acquired after 28 days of curing. Both the HPFRCC and normal concrete showed slightly higher strengths than the design compressive strength of 40 MPa. The compressive stress-strain relationships indicated that the HPFRCC was much more ductile than the normal concrete; the strain measured at failure was approximately 67% greater for the HPRCC. On the other hand, the secant modulus of elasticity of the normal concrete was about 24% greater than that of the HPFRCC. The secant modulus was calculated according to ACI 318-14, which is the slope of a line passing through 45% of the maximum compressive strength in the stress-strain curve.

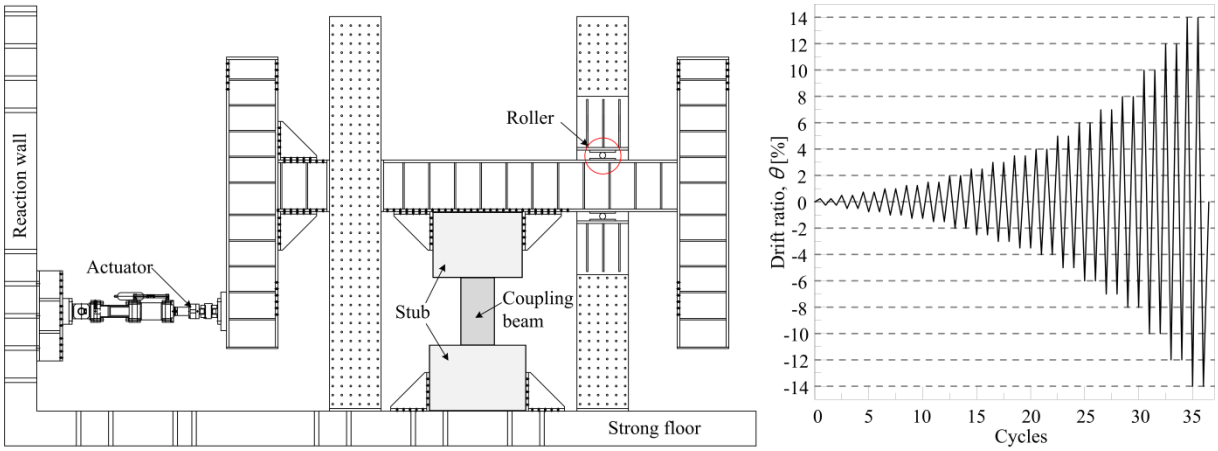

(a) (b)

Figure 2. Test setup and loading protocol.

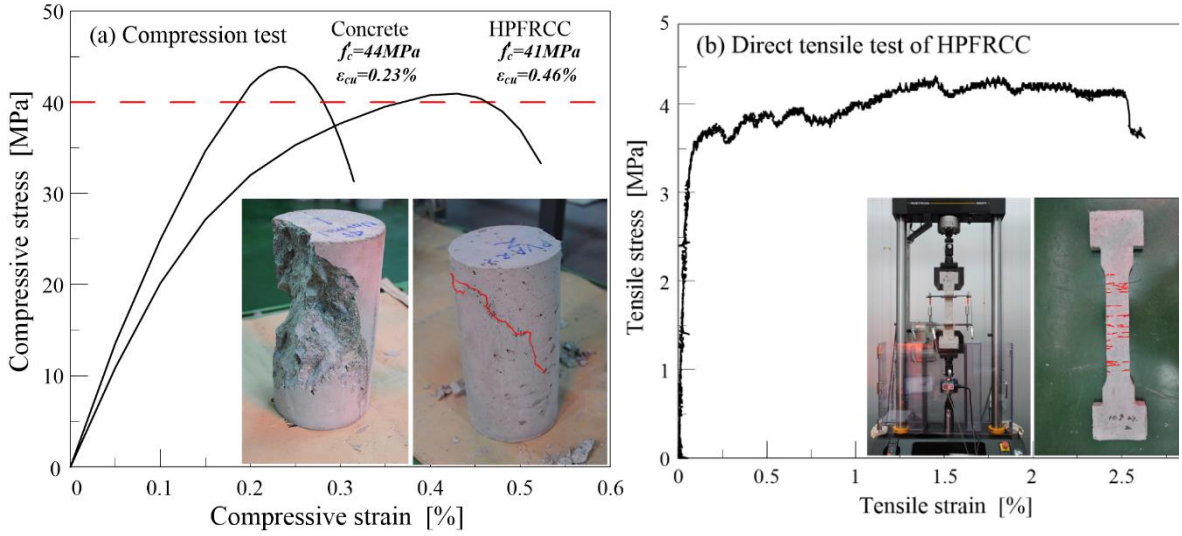

(a) Compression test (b) Direct tension test of HPFRCC

Figure 3. Stress-strain curves of concrete tests.

For direct tension tests, three dog-bone shaped specimens were fabricated, similar to those used by the

University of Michigan research group (Parra-Montesinos 2005). Two LVDTs in parallel were mounted along the sides of the specimen to estimate the average tensile strain, with the gage length of approximately 180 mm.

Fig. 3b shows the tensile stress-strain curve and cracking pattern of the HPFRCC used in this study. Under tension, the HPFRCC specimens showed ductile behavior by means of strain hardening, developing numerous well-distributed micro-cracks with the effect of fiber bridging [13, 15, 16]. The maximum tensile strain exceeded 2.5%, and the tensile strength was approximately 4.3 MPa. Table 2 summarizes the compressive and tensile strengths of the HPFRCC and normal concrete measured at the curing age of 28 days. Table 3 summarizes the mechanical properties of steel acquired from the tension tests.

Table 2. Properties of normal concrete and HPFRCC

Type	Compressive strength f_{cu} (MPa)	Maximum compressive strain ε_{cu} (%)	Direct tensile Stress (MPa)	Maximum tensile Strain (%)
Normal concrete	44	0.23	-	-
HPFRCC	41	0.46	4.3	2.5

Table 3. Properties of normal concrete and HPFRCC

Type	Compressive strength f_{cu} (MPa)	Maximum compressive strain ε_{cu} (%)	Direct tensile Stress (MPa)	Maximum tensile Strain (%)
Normal concrete	44	0.23	-	-
HPFRCC	41	0.46	4.3	2.5

3. Test Results and Observations

3.1 Load-displacement responses

Figure 4 shows the cyclic shear-drift responses of the coupling beam specimens. The right side vertical axis of this figure indicates the normalized shear stress, namely, the ratio of shear force in the coupling beam, taken equal to the actuator load, to the product of the beam cross-sectional area (A_{cw}) and the square root of the concrete compressive strength (f'_c). Table 4 summarizes the yield load (V_y), yield drift ratio (θ_y), maximum load (V_u), maximum drift ratio (θ_u), and ductility ratio (μ) of each specimen. The yield and maximum drift ratios were determined according to the work of Pan and Moehle (1989). The yield drift ratio corresponds to the point of intersection between the secant line connecting the origin to the point of 2/3 of the maximum load and the horizontal line at the point of the maximum load. The maximum drift ratio was measured when the strength reduced to 80% of the maximum load. The ductility ratio is defined as the maximum drift divided by the yield drift.

Specimens RC-2.0 and RC-3.5 of normal concrete, composed of standard RC, having code-specified transverse reinforcement exhibited stable load-drift behavior up to about 4% and 8% drift respectively, without considerable drop in strength. Between the two, the slender beam specimen showed much more ductility and had full load-drift loops. The RC-2.0 specimen suffered significant and successive strength drops from the second cycle to 5% drift, when some diagonal and transverse reinforcement ruptured. In contrast, the higher-aspect-ratio specimen RC-3.5 sustained more than 80% of its maximum load up to the first positive loading cycle of 10% drift ratio. Thus, the ductility ratios of Specimens RC-2.0 and RC-3.5 for loading in the positive direction were approximately 3.0 and 5.7 in, respectively.

Specimens HC-2.0 and HC-3.5, composed of HPFRCC, having one half the amount of code-specified transverse reinforcement, showed load-drift responses that were generally similar to those of the

normal concrete specimens discussed above. HC-2.0 and HC-3.5 exhibited stable behavior up to 5% and 8% drift, respectively. HC-2.0 underwent large strength drops from the first cycle up to 6% drift, and completely collapsed during the 7% drift cycles, owing to rupture of the diagonal reinforcement. On the other hand, HC-3.5 started to become unstable only from the 10% drift cycles. The ductility ratios of Specimens HC-2.0 and HC-3.5 for loading in the positive direction were approximately 3.7 and 5.6, respectively.

It is noted that the normalized shear stress greatly exceeded the design limit of 0.83 for diagonally reinforced coupling beams as specified in ACI 318-14. Therefore, the test results suggest that bundled diagonal reinforcement was applicable in both deep and slender coupling beams, and that the HPFRCC was effective in allowing the amount of transverse reinforcement required by ACI 318-14 to be reduced by half.

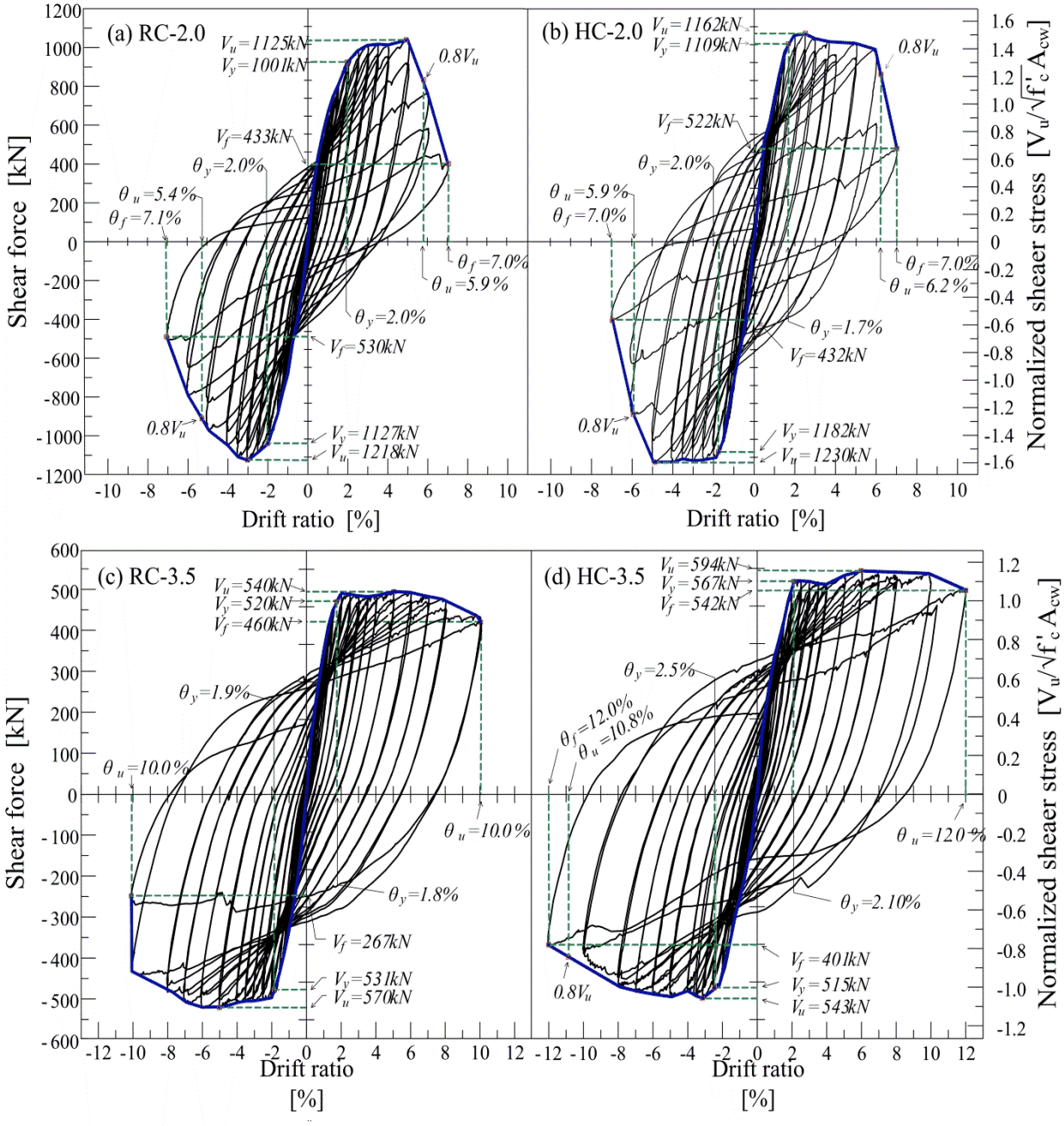

Figure 4. Hysteretic shear-drift responses.

Table 4. Test results for critical strengths and drift ratios

Specimen		V_y (kN)	θ_y (%)	V_u (kN)	θ_u (%)	μ (θ_u/θ_y)	V_{n-ACI} (kN)	M_{n-ACI} (kN-m)
RC-2.0	(+)	1001	1.98	1125	5.88	2.96	490	259
	(−)	1127	2.00	1218	5.37	2.68	490	259
HC-2.0	(+)	1109	1.70	1162	6.24	3.67	490	259
	(−)	1182	1.76	1230	5.88	3.34	490	259
RC-3.5	(+)	532	1.76	540	10.04	5.70	316	167
	(−)	531	1.88	570	10.02	5.34	316	167
HC-3.5	(+)	567	2.15	594	12.02	5.60	316	167
	(−)	515	2.53	543	10.79	4.27	316	167

Note: V_y = yield load; V_u = maximum load; θ_y = yield drift ratio; θ_u = maximum drift ratio; μ = ductility ratio equal to θ_u / θ_y; V_{n-ACI}, M_{n-ACI} = shear and moment strength calculated by ACI 318-11 (ACI 2014)

Figure 5 shows the envelopes of the cyclic shear-drift response curves for the four coupling beam specimens. Among both pairs of specimens with the same aspect ratio, the RC and HPFRCC specimens not only achieved similar maximum loads, but also underwent similar strength degradation histories. In addition, the primary cause of sudden strength drops in all four specimens was the rupture of diagonal reinforcement with no buckling. Therefore, combining the use of HPFRCC and half the amount of code-required transverse steel appeared to provide confinement equivalent to that of the code-required transverse reinforcement.

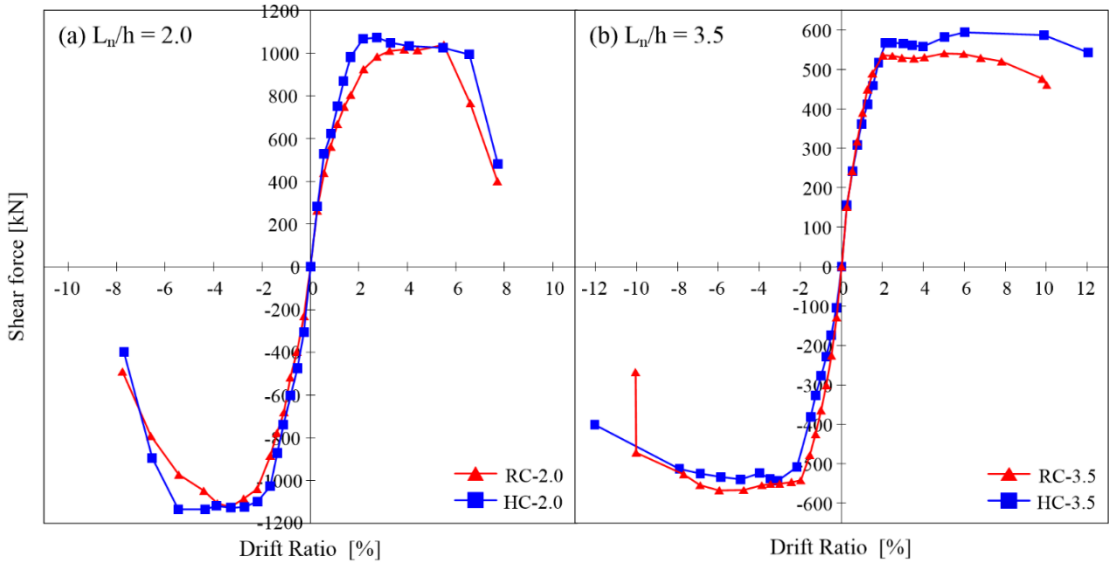

Figure 5. Envelope curves.

4. Conclusions

In this study, HPFRCC and RC coupling beam specimens with bundled diagonal reinforcement were tested under cyclic lateral loading in order to assess the effectiveness of HPFRCC. The RC specimens were reinforced with the code-required amount of transverse steel per ACI 318-14, whereas the HPFRCC specimens were reinforced with about half the code-required amount of transverse steel.

The HPFRCC coupling beams had similar lateral strengths to those of the RC coupling beams and

superior seismic capacities, even though the HPFECC specimens were reinforced using only half the code-required amount of transverse steel. This suggests that the amount of transverse reinforcement required by ACI 318-14 could be reduced by half with the use of HPFRCC, which supplied adequate confinement for the bundled diagonal bars.

The maximum drift ratio achieved was at least about 5.37 and 10.0 in the specimens of aspect ratios 2.0 and 3.5, respectively. Also, no substantial strength drop occurred until the bundled diagonal bars ruptured in all specimens. This indicates that the use of bundled diagonal reinforcement was effective in ensuring suitable seismic performances of both deep and slender coupling beams; this design also enables simplified construction.

5. Reference

[1] Berg VB and Stratta JL 1964 Anchorage and the Alaska Earthquake of March 27, 1964, AISC.
[2] Paulay T and Priestley MJ 1992 Seismic design of reinforced concrete and masonry buildings, John Wiley & Sons, N.Y.
[3] Paulay T and Binney JR 1974 Diagonally reinforced coupling beams of shear walls. Amer. Conc. I., 42, 579-598.
[4] Tassios TP, Moretti M and Bezas A 1996 On the behavior and ductility of reinforced concrete coupling beams of shear walls. ACI Struct. J., 93(6), 711-720.
[5] Galano L and Vignoli A 2005 Seismic behavior of short coupling beams with different reinforcement layouts. ACI Struct. J., 97(6), 876-885.
[6] Fortney PJ, Rassati GA and Sharooz BM 2008 Investigation on effect of transverse reinforcement on performance of diagonally reinforced coupling beams. ACI Struct. J., 105(6), 781-788.
[7] Harries K. A., Fortney P. J., Shahrooz B. M., and Brienen P. J. (2005). "Practical design of diagonally reinforced concrete coupling beams-critical review of ACI 318 requirements." ACI Struct. J., 102(6), 876-882.
[8] ACI (American Concrete Institute). (2014). Building code requirements for structural concrete. ACI 318-14, Farmington Hills, MI, USA.
[9] Han SW, Lee CS, Shin M and Lee K 2015 Cyclic performance of precast coupling beams with bundled diagonal reinforcement. Eng. Struct., 93, 142-151.
[10] Canbolat BA, Parra-Montesinos GJ and Wight JK 2005 Experimental study on seismic behavior of high-performance fiber-reinforced cement composite coupling beams. ACI Struct. J., 102(1),159-166.
[11] Parra-Montesinos GJ 2005 High-performance fiber-reinforced cement composites: an alternative for seismic design of structures. ACI Struct. J., 102(5), 668-675.
[12] Parra-Montesinos GJ, Peterfreund SW and Chao SH 2005 Highly damage-tolerant beam-column joints through use of high-performance fiber-reinforced cement composites. ACI Struct. J., 102(3), 487-495.
[13] Naaman AE, Likhitruangsilp V and Parra-Montesinos GJ 2007 Punching shear response of high-performance fiber-reinforced cementitious composite slabs. ACI Struct. J., 104(2), 170-179.
[14] Shin M, Gwon SW, Lee K, Han SW and Jo YW 2014 Effectiveness of high performance fiber-reinforced cement composites in slender coupling beams. Constr. Build. Mater., 68, 476-490.
[15] Li VC 2003 On engineered cementitious composites (ECC). J. Adv. Concr. Technol., 1(3), 215-230.
[16] Yang EH and Li VC 2010 Strain-hardening fiber cement optimization and component tailoring by means of a micromechanical model. Constr. Build. Mater., 24(2), 130-139.

Acknowledgement

A The research was supported by grants from the National Research Foundation of Korea (NRF-2017R1A2B3008937).